Chapter 5

Antibacterial and Cellular Response of HA, $BaTiO_3$ (BT), $CaTiO_3$ (CT), $Na_{0.5}K_{0.5}NbO_3$ (NKN) and Their Composites

This chapter discusses the effect of incorporation of piezoelectric NKN, BT and perovskite CT as secondary phases on antibacterial and cellular response of HA-based composites. In addition, the combined effect of inclusion of piezoelectric NKN, BT and perovskite CT as a secondary phases in the HA matrix as well as surface polarization on antibacterial and cellular response have been examined. Additionally, the enzymatic activities such as superoxide dismutase, catalase, lipoperoxide, and total protein estimation have also been examined to understand the mechanisms, responsible for such antibacterial response.

5.1 XRD analysis

The XRD patterns of sintered HA, BT, CT, NKN, and their composites are represented in Fig.5.1. The single phase HA (JCPDS no. 09-0432), BT (JCPDS no. 74-2491), CT (JCPDS no. 82-0228) and NKN (JCPDS no. 77-038) are observed. The XRD patterns of sintered HA, BT, CT and NKN were analyzed using X-pert high score software. The XRD for HA-30 NKN, HA-30 BT and HA-30 CT composites reveal the combination of distinct peaks for HA, NKN, BT and CT phases without any dissociation/ reaction between constituent phases.

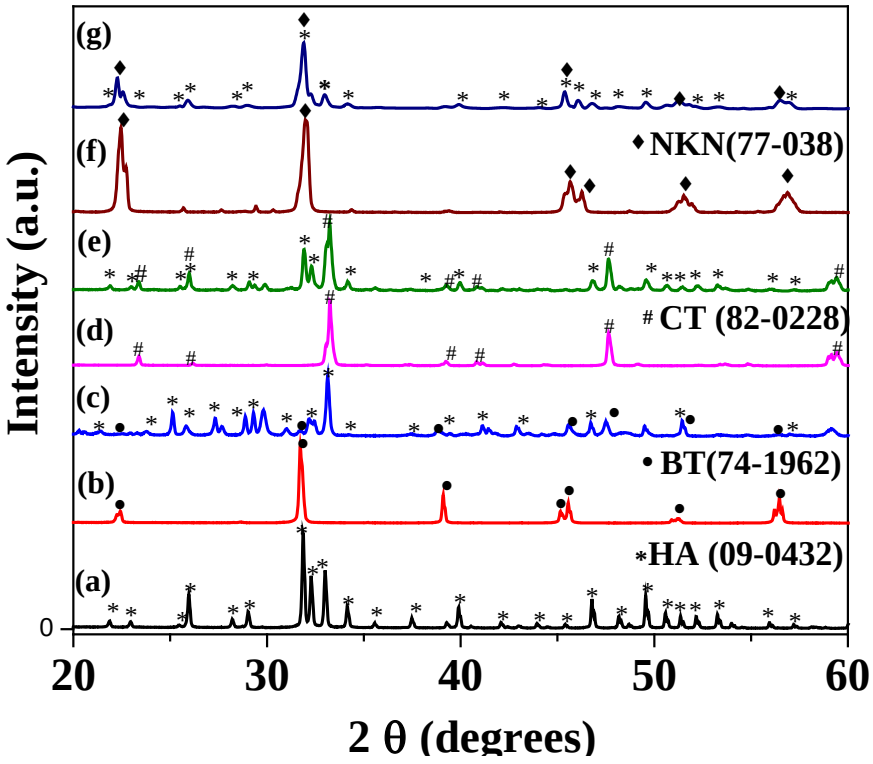

Fig. 5.1 The X-ray diffraction patterns for sintered (a) HA, (b) BT, (c) HA-30 vol. % BT, (d) CT, (e) HA-30 vol.% CT, (f) NKN and (g) HA-30 vol. % NKN composites.

5.2. Fourier transform infrared spectroscopic analysis

Fig. 5.2 represents the FTIR spectra of sintered HA, BT, CT, NKN, HA-30 BT, HA-30 CT and HA-30 NKN composites. The FTIR spectra of HA [Fig. 5.2 (a)] shows the broad band at 3572 cm^{-1} and 630 cm^{-1}, which corresponds to OH^- stretching and bending vibrations, respectively [1]. The vibrations of PO_4^{3-} group appears at 1089, 1026, 962, 604, and 563 cm^{-1} [2].The absorption band appears at 1415 and 1450 cm^{-1} corresponds to $CO^2{}_3^-$ group [3]. The FTIR spectra of BT [Fig. 5.2 (b)] represent the broad bands at 592 and 452 cm^{-1} which correspond to Ti-O stretching and bending vibrations, respectively [4]. The small peaks, corresponding to OH^- stretching and bending vibrations are observed at ~ 3367 and 1630 cm^{-1}, respectively [5]. The vibration of Ba-O band is observed at ~ 431 cm^{-1} [6]. Fig. 5.2 (d) illustrates the FTIR spectrum of CT. The

characteristic bands appear at ~ 449 and 546 cm^{-1}, which corresponds to the stretching of Ti-O [7]. The band, observed at ~ 570 cm^{-1} represents the characteristic peak of Ca-TiO. The FTIR spectra of NKN represent the presence of characteristic peak of NbO at 524 cm^{-1} [Fig. 5.2 (f)]. The obtained FTIR spectra for HA-30 BT, HA-30 CT, and HA-30 NKN composites [Fig. 5.2 (c), (e), and (g)] shows the combination of individual bands, corresponding to OH^-, Ti-O, PO_4^{3-}, CO_3^{2-}, Ba-O, Ca-TiO, and NbO.

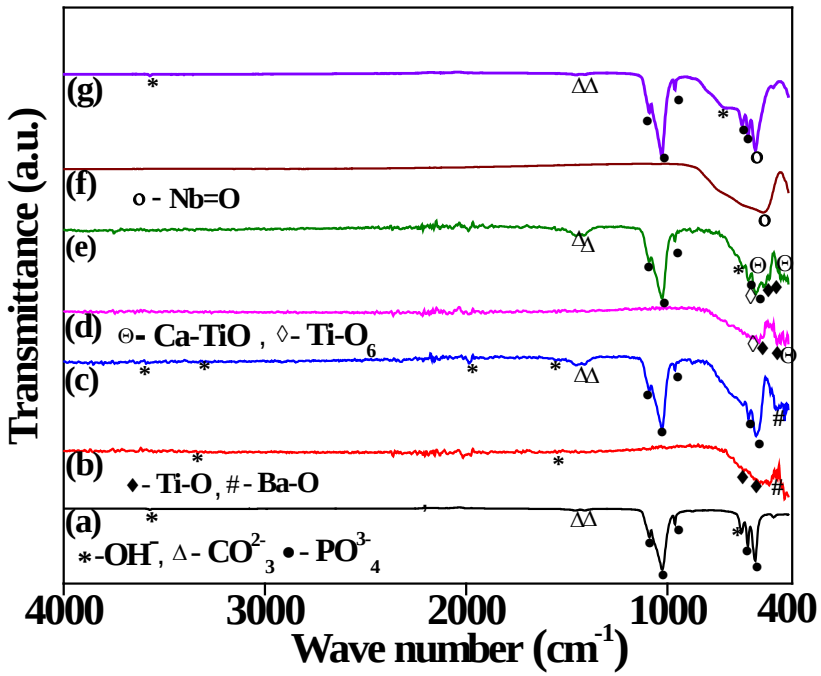

Fig. 5.2. Fourier transform infra-red (FTIR) spectra of sintered (a) HA, (b) BT, (c) HA-30 vol. % BT, (d) CT, (e) HA-30 vol.% CT, (f) NKN and (g) HA-30 vol. % NKN composites.

5.3. Surface morphology

Fig. 5.3 represents the scanning electron microscopy (SEM) images of fractured HA, NKN, BT, CT, HA-30 NKN, HA- 30 BT, and HA-30 CT composite surfaces. The average grain size of fractured HA, NKN, BT, CT HA-30 NKN, HA- 30 BT and HA-30

CT composites were measured to be 1.02 ± .05, 0.94 ± .10, 0.65 ± 0.10, 0.84 ± .11, 0.97 ± 0.10, 0.96 ± 0.11 and

0.92 ± 0.10 μm, respectively. The energy dispersive X-ray (EDX) analyses show the presence of corresponding elements (Ca, P, O, Na, K, Nb, Ba, and Ti) in the samples.

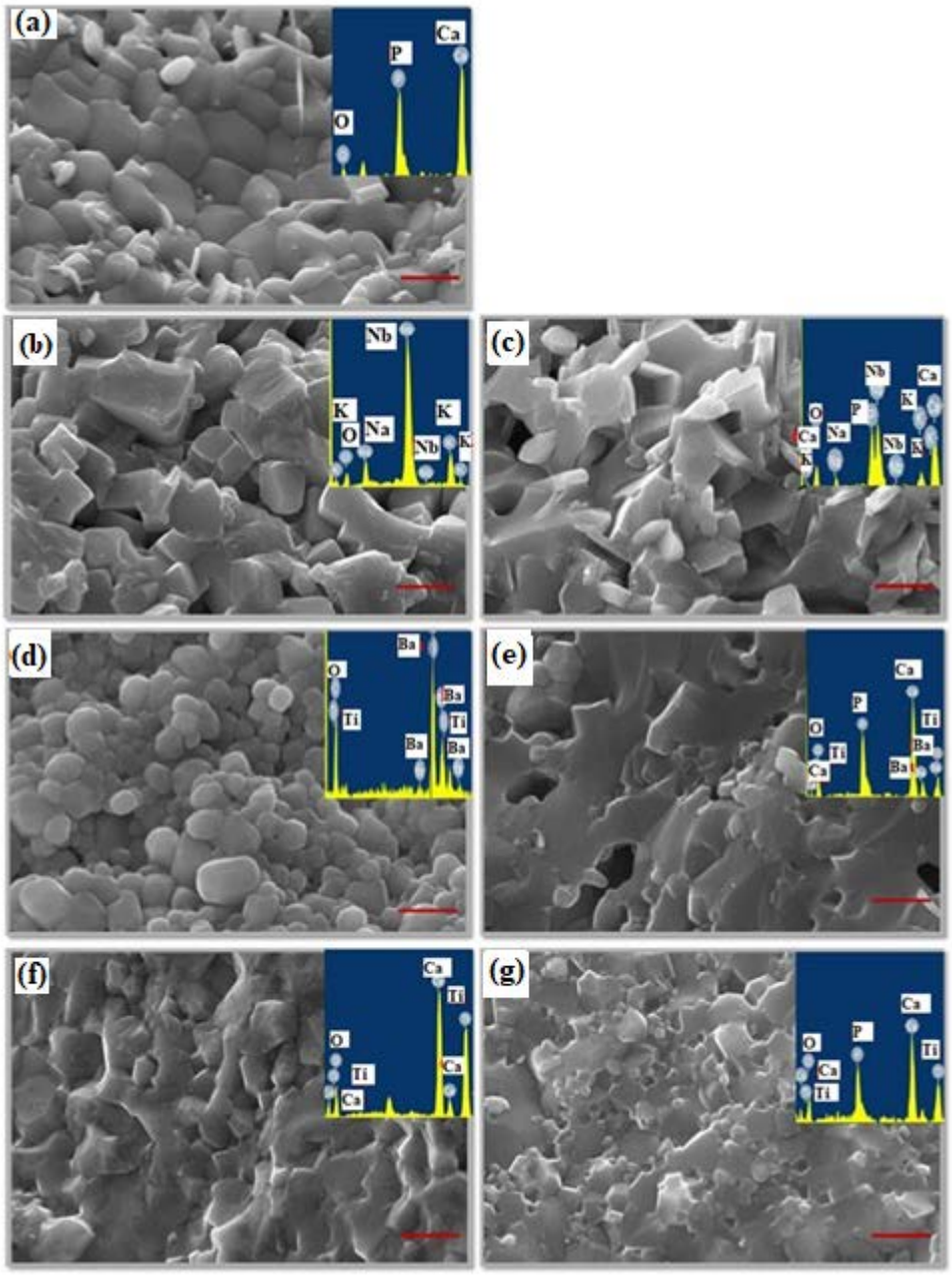

Fig.5.3. Scanning electron micrographs of fractured surfaces of (a) HA,(b) NKN, (c) HA-30 vol. % NKN (d) BT, (e) HA-30 vol. % BT, (f) CT and (g) HA-30 vol. % CT (scale bar corresponds to 1 μm).

5.4. Contact angle measurement

Figs. 5.4 (a) and (b) represent contact angle, measured with deionized water droplet and culture media, respectively. It is observed that the contact angle of unpolarized HA and HA-30 NKN, HA-30 BT and HA-30 CT composites are almost similar (~56^{o}) which represents that the wettability of prepared composites remains unchanged with addition of secondary phases. The contact angle of N-polarized surfaces measured on both, deionized water droplet and culture media are observed to be lower as compared to unpolarized surface of the same composition. Among all samples, N-polarized CT and HA-30 CT composite reflect the lowest contact angle. These results clearly demonstrate that polarization increases the hydrophilicity of surfaces.

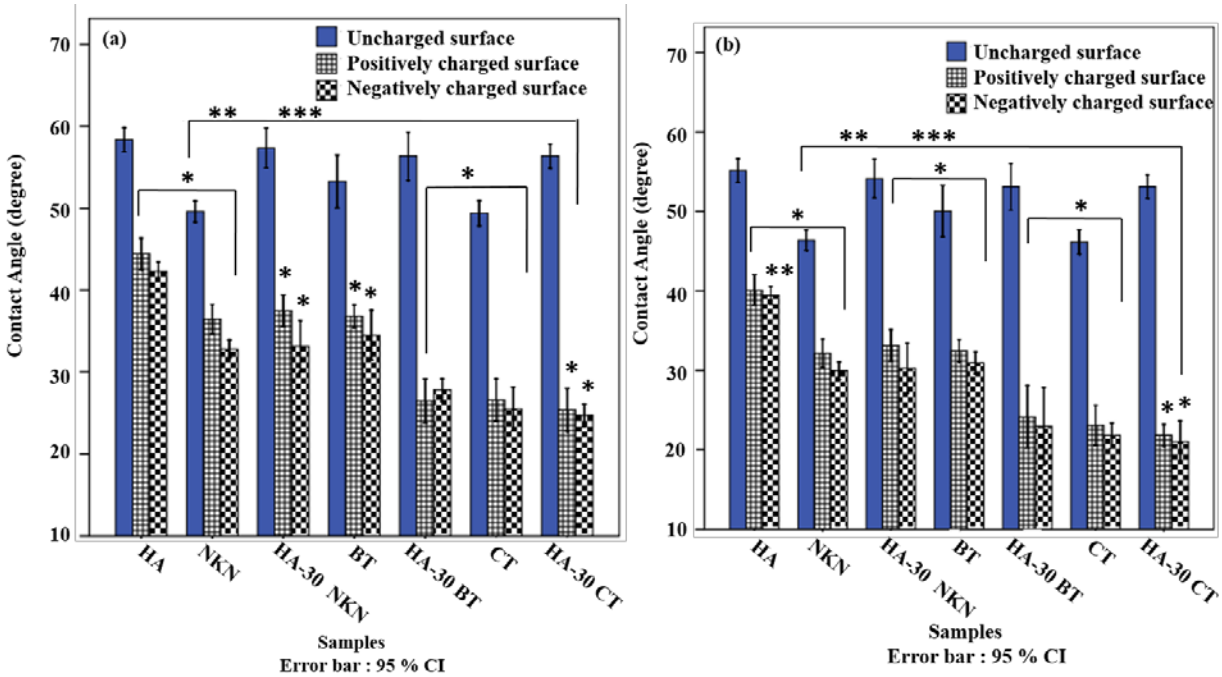

*Fig.5.4. Contact angle values of (a) deionized water and (b) culture media on unpolarized and polarized HA, NKN, BT, CT, and HA-30 BT, HA-30 NKN, HA-30 CT composites. All the samples show the statistically significant difference with unpolarized HA, at p < 0.05 (represented as *). The symbols (**) and (***) reflect the statistically significant difference among the samples while comparing with N-polarized and P-polarized HA, at p < 0.05, respectively.*

5.5. Antibacterial response

5.5.1. MTT assay

Fig.5.5. represents the MTT assay results of *E. coli* and *S. aureus* bacteria, while cultured on unpolarized and polarized sample surfaces. The incorporation of piezoelectric BT, NKN and perovskite CT as secondary phases in HA matrix increases the antibacterial response of HA. Among the unpolarized samples, the piezoelectric BT and NKN samples demonstrate better antibacterial property. The statistical analyses reveal that all the unpolarized as well as polarized samples exhibit significant reduction in the optical density for both the bacteria [represented as (*) in Fig. 5.5]. The optical density of all the cultured samples is significantly lower than that of N-polarized HA. However, in contrast to P-polarized HA, viability of both the bacteria decreases significantly for all the samples, except unpolarized HA-30 BT, NKN for *E. coli* bacteria and unpolarized HA-30 BT for *S. aureus* bacteria. The viability of *E. coli and S. aureus bacteria* on unpolarized NKN, BT and CT surfaces are reduced to approximately (19, 37, 32 %) and (24.8, 42, 20 %), respectively, as compared to unpolarized HA. The inclusion of 30 vol. % of NKN, BT and CT in HA matrix decreases the viability of *E. coli* and *S. aureus* bacteria by (29, 30, 16 %) and (13.5, 25.4, 24 %), respectively. Furthermore, it is observed that polarization reduces the total number of viable cells for both the bacteria. Among all the samples, N-polarized and P-polarized BT surface reduces the viability of E. *coli* and *S. aureus* bacteria by ~ 56.6 and 60.7 %, respectively. The N-polarized surfaces reduce more *E. coli* bacteria. However, P-polarized surfaces offer significant reduction in the viability of *S. aureus* bacteria. Overall, the MTT results confirmed that the addition of 30 vol. % piezoelectric BT, NKN and perovskite CT in HA, and polarization treatment notably enhances its antibacterial response.

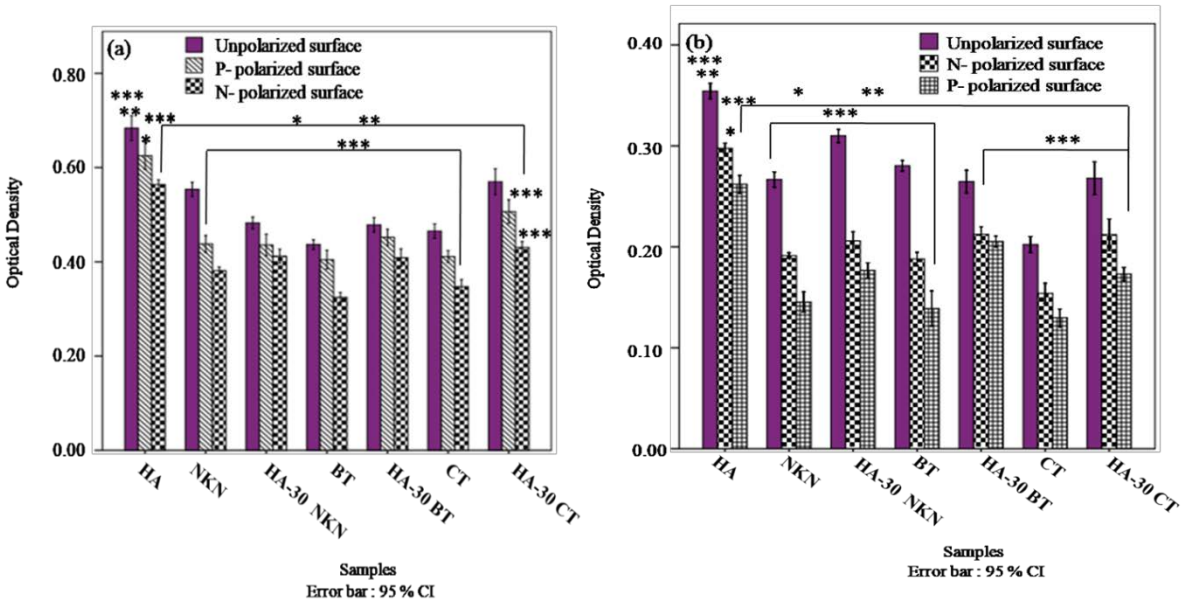

*Fig. 5.5. The viability of (a) E. coli and (b) S. aureus bacteria, while cultured on HA, NKN, BT, CT, and HA-30 vol. % BT, HA-30 vol. % NKN, HA-30 vol. % CT composites. All the samples show the statistically significant difference with unpolarized HA, at $p < 0.05$ (represented as *). The symbols (**) and (***) reflect the statistically significant difference among the samples while comparing with N-polarized and P-polarized HA, at $p < 0.05$, respectively.*

5.5.2. Colony counting method

The antibacterial response of unpolarized and polarized samples was examined qualitatively for both, *E. coli* and *S. aureus* bacteria using colony counting method according to ASTM E-3031-15 standard. The freshly prepared culture media was diluted using serial dilution method and unpolarized as well as polarized samples were seeded with 100 µL diluted (three fold dilution) culture in 24 well plate and incubated for 8 h at 37 ºC. After incubation, the samples were transferred in test tube for ultrasonication. The samples were ultrasonicated in 1x PBS for 5 min and the solution was diluted 1000 times with media.

To observe the colony formation unit (CFU), 100 µL diluted culture was spreaded in agar plates using L rod and incubated further for 8 h at 37 ºC. The bacterial colonies

were counted using digital colony counter. To understand the effect of polarization on bacterial cells, log reduction bacterial colonies for each sample were calculated as [8],

$$\mathbf{Log_{10}\ reduction} = \mathbf{C} - \mathbf{T} \qquad (\mathbf{5.1})$$

Where, C and T are the geometric mean of control and treated samples (unpolarized and polarized), respectively. According to ASTM E3031-15 standard, if Log_{10} reduction = Log_{10} control, the sample is bacteriostatic. If Log_{10} reduction > Log_{10} control, the sample is bactericidal and if Log reduction < Log control > 0.5, the samples partially inhibit the bacterial growth. In addition, the antibacterial ratio for both the bacteria, cultured on unpolarized and polarized samples were calculated as [9],

$$\mathbf{Antibacterial\ ratio}\ (\%) = \frac{\mathbf{A} - \mathbf{B}}{\mathbf{A}} \times \mathbf{100} \qquad (\mathbf{5.2})$$

Where, A and B represent the CFU in blank and developed samples, respectively.

Figs. 5.6 (a) and (b) represent the colonies of *E. coli* and *S. aureus* bacteria, while cultured on unpolarized and polarized HA, NKN, BT, CT, HA-30 NKN, HA-30 BT and HA-30 CT composites, respectively. It is clearly observed that piezoelectric NKN, BT and perovskite CT samples demonstrate lower bacterial colonies as compared to HA, which suggests the antibacterial nature of NKN, BT and CT samples as compared to HA. Similarly, the composites HA-30 NKN, HA-30 BT and HA-30 CT demonstrate reduction in bacterial colonies as compared to HA. In addition, the colonies of *E. coli* bacteria on N-polarized surfaces decrease as compared to unpolarized and P-polarized surfaces, for all the compositions. However, for *S. aureus* bacteria, P-polarized surfaces demonstrate lower bacterial colonies as compared to unpolarized and N-polarized surfaces.

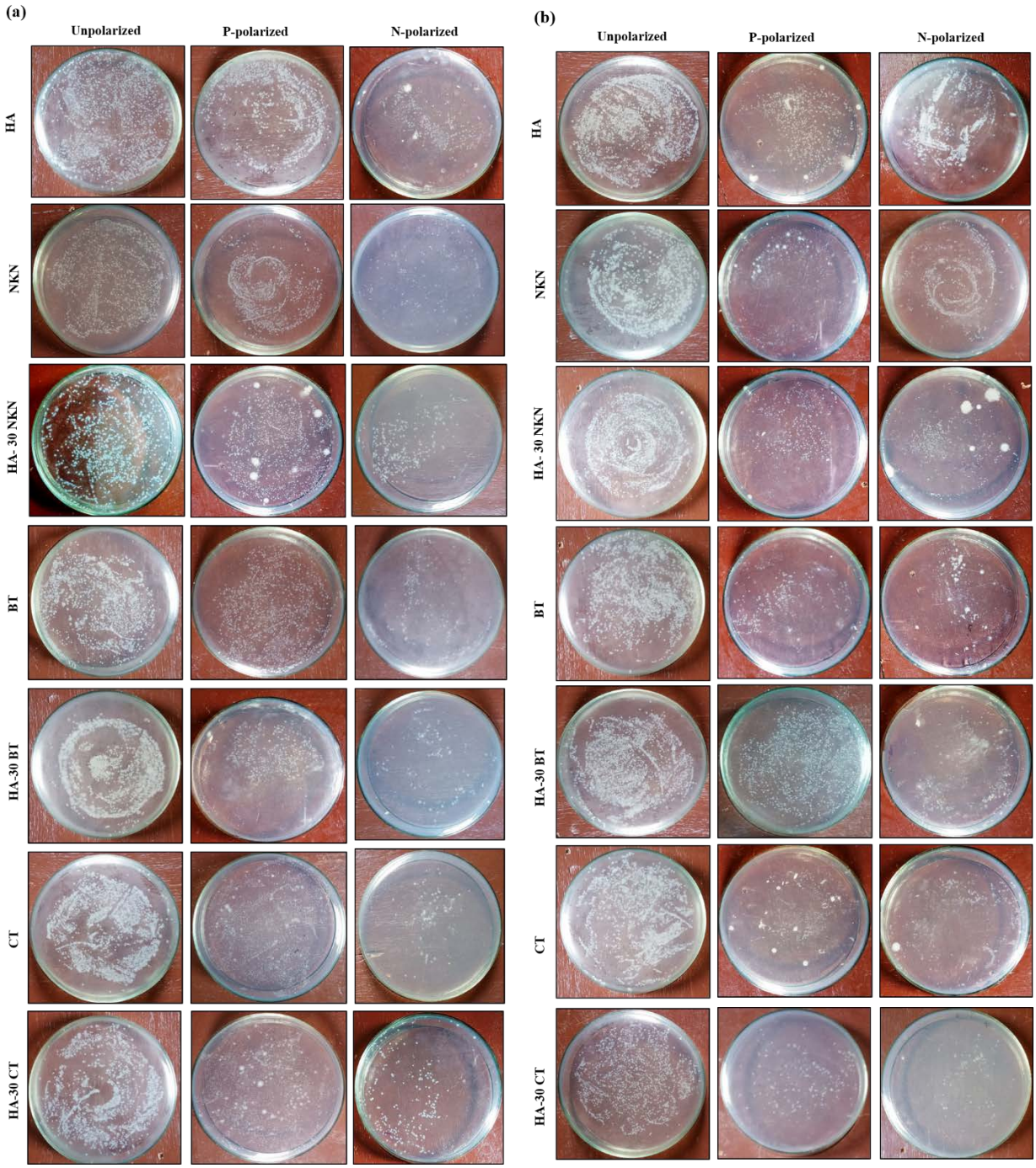

Fig.5.6. Digital camara images, representing the colonies of viable (a) E. coli and (b) S. aureus bacteria, respectively, cultured for 8 h on unpolarized and polarized HA, NKN, BT, CT, HA- vol. % 30 NKN, HA-30 vol. % BT and HA- 30 vol. % CT composites.

Figs. 5.7 (a) and (b) represent the Log_{10} reduction per unit area with sample composition for *E. coli* and *S. aureus* bacteria, respectively. It is clearly observed that positively polarized NKN, BT and CT samples demonstrate higher values (than that control) for

both the bacteria. Higher values for these samples suggest the bactericidal nature of P-polarized NKN, BT and CT samples. In addition, the unpolarized and N-polarized samples demonstrate higher Log_{10} reduction values as compared to unpolarized HA and lower to control samples which suggest that these samples have partially inhibited the bacterial growth.

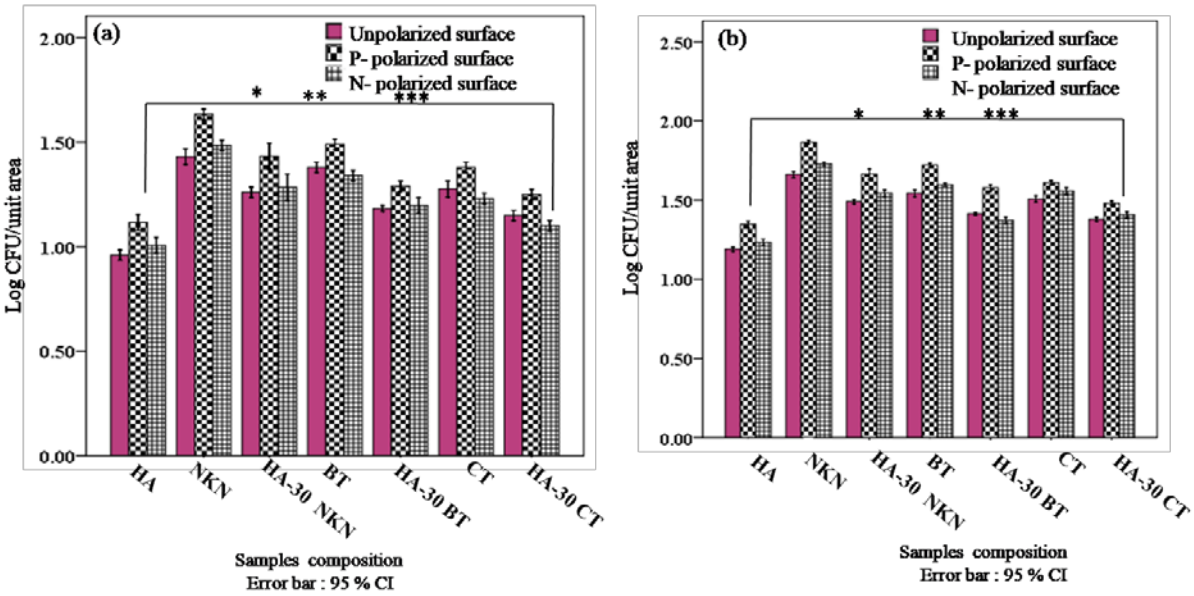

*Fig 5.7. Log10 CFU/unit area for (a) E. coli and (b) S.aureus bacteria, while cultured on HA, NKN, BT, CT, HA-30 vol. % NKN, HA-30 vol. % BT and HA-30 vol. % CT composites. All the samples show the statistically significant difference with unpolarized HA, at $p < 0.05$ (represented as *). The symbols (**) and (***) reflect the statistically significant difference among the samples while comparing with N-polarized and P-polarized HA, at $p < 0.05$, respectively.*

5.5.3. Antibacterial ratio

The antibacterial ratio for both, *E. coli* and *S. aureus* bacteria, while cultured on unpolarized and polarized samples are represented in Figs. 5.8 (a) and (b), respectively. The antibacterial ratio for *E. coli* and *S. aureus* bacteria are observed to be higher for piezoelectric NKN, BT and CT samples as compared to HA i.e, the addition of piezoelectric NKN, BT and CT as secondary phases in HA matrix increases the

antibacterial ratios for both the bacteria. The statistical analyses reveal that the antibacterial ratios of both, *E. coli* and *S. aureus* bacteria significantly increase on unpolarized and polarized samples as compared to unpolarized HA [represented as (*) in Fig. 5.8)]. However, all polarized samples show significant increase in the antibacterial ratio with respect to N-polarized and P-polarized surfaces of HA, for both, E. coli and *S. aureus* bacteria [represented as (**) and (***) in Fig. 5.8]. Overall, the antibacterial ratio for *E. coli* and *S. aureus* bacteria, while cultured on unpolarized and polarized HA, NKN, BT, CT, HA-30 NKN, HA-30 BT and HA-30 CT composites samples, demonstrate similar results, as observed by MTT assay.

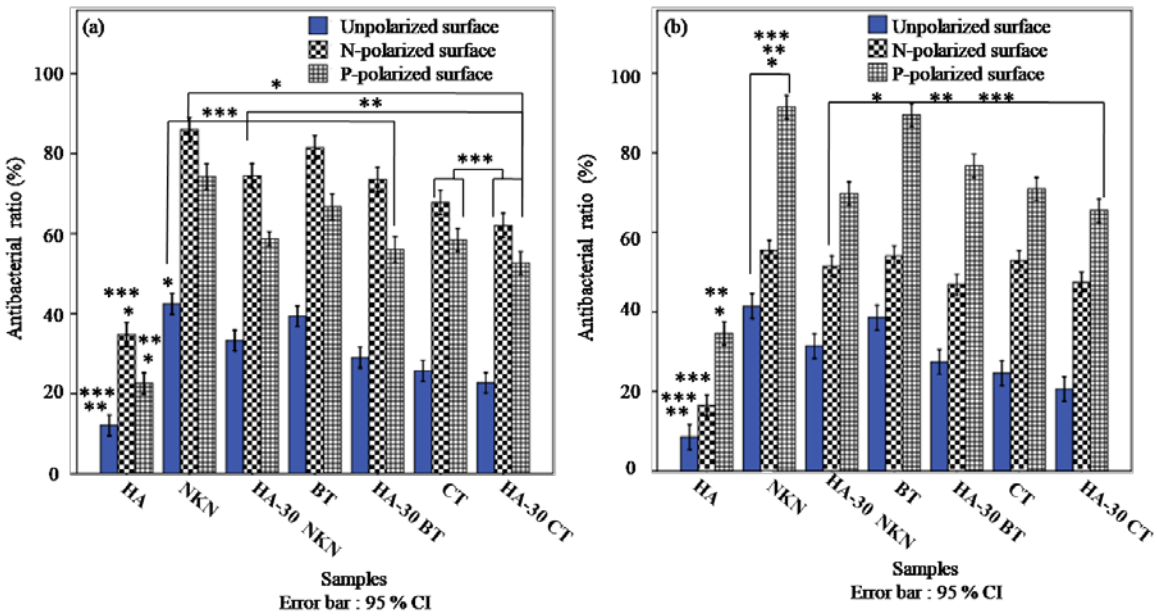

Fig. 5.8. The antibacterial ratios for (a) E.coli and (b) S.aureus bacteria, cultured on unpolarized and polarized HA, NKN, BT, CT, HA-30 NKN, HA-30 BT and HA- 30 CT composites. The symbol (*) represents the statistically significant difference among all samples with respect to unpolarized HA, at $p < 0.05$. The symbols (**) and (***) represent the statistically significant difference among all the samples with respect to N-polarized and P-polarized HA, respectively, at $p < 0.05$.

5.5.4 Live/dead assay

Figs. 5.9 and 5.10 represent the populations of live and dead bacteria, adhered on HA, NKN, BT, CT, HA-30 NKN, HA-30 BT, HA-30CT composite surfaces, respectively. The unpolarized HA shows higher number of live *E. coli* as well as *S. aureus* bacteria. The number of dead bacterial cells (red spot) increases with the addition of NKN, BT, and CT in HA matrix for both, the bacteria as compared to unpolarized HA.

The positively polarized surfaces demonstrate higher dead cells for both, *E. coli* and *S. aureus* bacteria. Overall, the inclusion of BT, NKN and CT as well as polarization (P-polarized surface) reduces the bacterial population.

The interaction of both, *E. coli* and *S. aureus* bacteria with unpolarized and polarized surfaces depends upon the charge polarity of surface as well as bacteria [10]. It has been reported that both, *E. coli* and *S. aureus* bacteria possess negative charge due to the outer layer of lipopolysaccharides and thick layer of peptidoglycan, respectively [11]. The *E. coli* bacteria exhibit more negative charge as compared to *S. aureus* bacteria. Kłodzińska et al [12] also reported that the zeta potentials of *E. coli* and *S. aureus* bacteria are -49 and -31.7 mV, respectively. The electrostatic interaction can take place between polarized surface and bacterial cells. Also, the polarization increases the hydrophilicity of the surfaces, which reduces the adhesion of bacterial cells [13]. Therefore, the population of *E. coli* and *S. aureus* bacteria reduces on polarized surfaces. The polarized surfaces generate a micro electric field [14]. This electric field generates more ROS such as H_2O_2, OH^-, and O_2^- etc., P-polarized surface [15]. These free radicals diffuse into the cell wall and damage the outer layer of bacterial cells like, lipopolysaccharides and peptidoglycan for *E. coli* and *S. aureus* bacteria, respectively and produce the oxidative stress [16]. The excess amount of ROS, produced on the polarized surfaces can damage

the DNA and proteins in the bacterial cells, which lead to the death of bacterial cells (as summarized in Fig. 5.18).

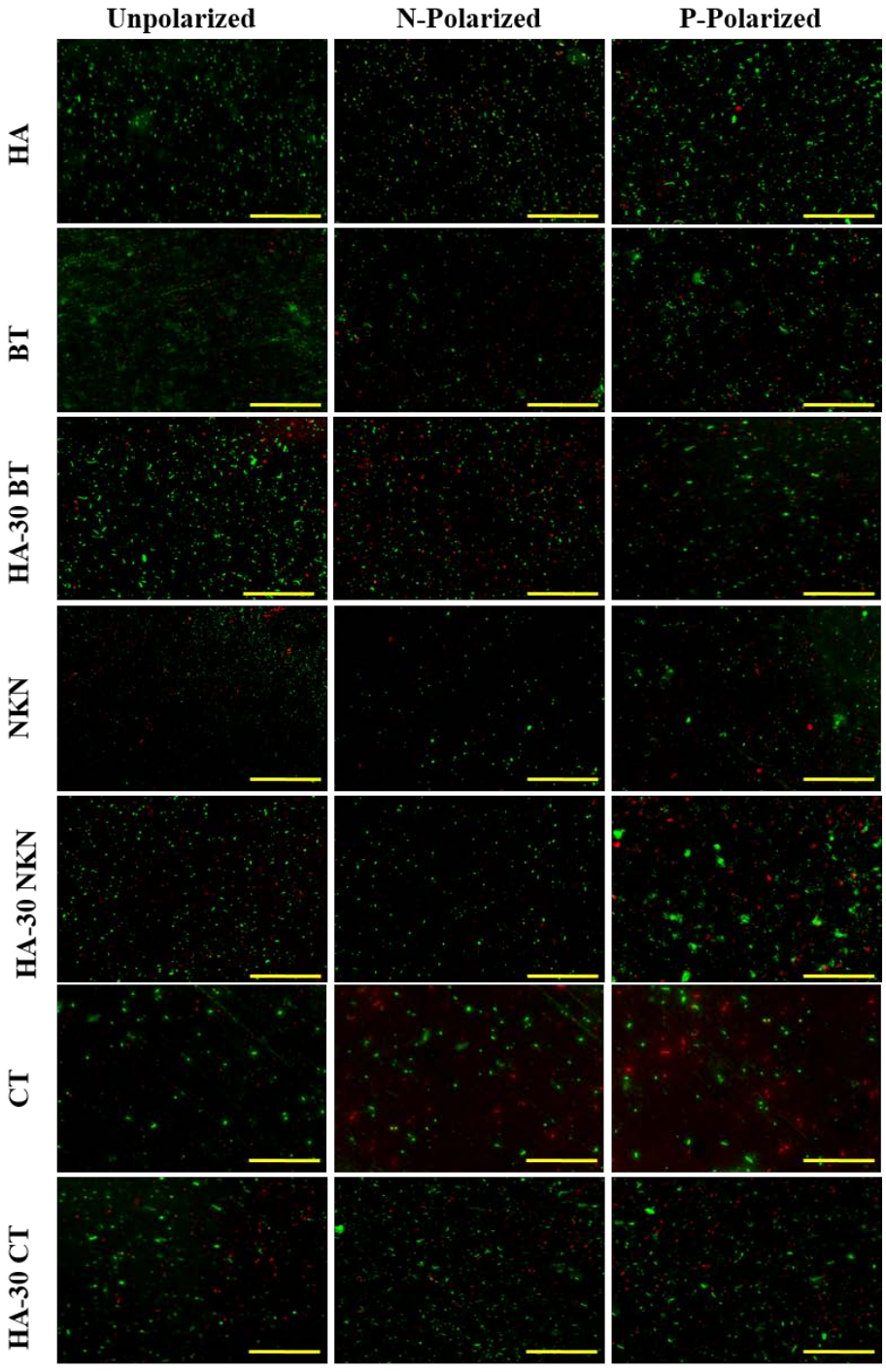

Fig. 5.9. Fluorescent microscopy images of live and dead E. coli bacteria, while cultured on HA, NKN, BT, CT, and HA-30 vol. % BT, HA-30 vol. % NKN, HA-30 vol. % CT composites (scale bar corresponds to 100 µm).

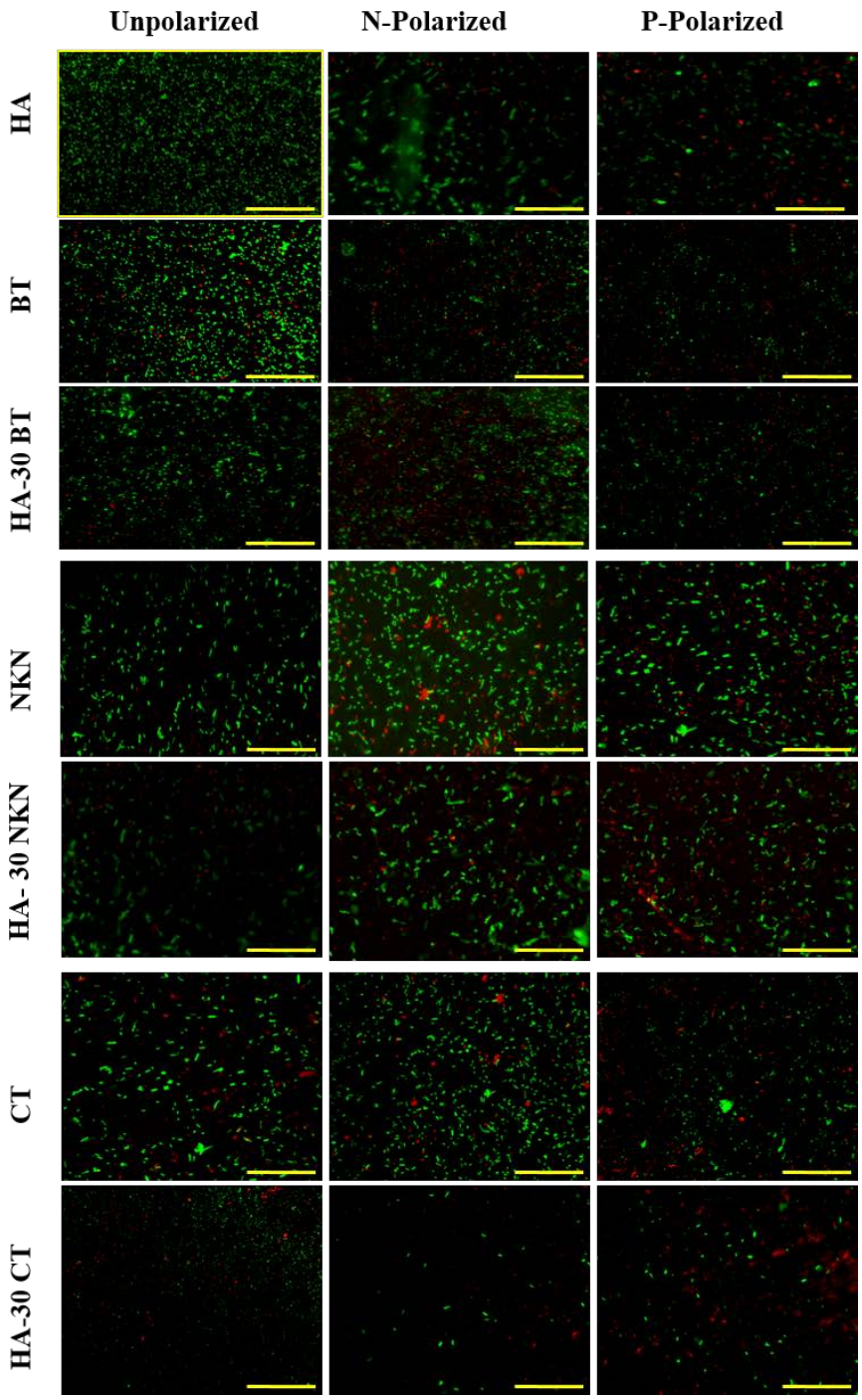

Fig. 5.10. Fluorescent microscopy images of live and dead S.aureus bacteria, while cultured on HA, NKN, BT, CT, and HA-30 vol. % BT, HA-30 vol. % NKN, HA-30 vol. % CT composites (scale bar corresponds to 100 µm).

5. 6. Enzymatic activity

The effect of enzymatic activity such as superoxide assay, catalase assay, lipoperoxide assay and protein estimation towards antibacterial response of unpolarized and polarized sample surface were examined.

5.6.1. Superoxide dismutase assay

The SOD assay was used to quantify the antioxidant enzymes such as, super oxides (O_2^-), produced on unpolarized and polarized sample surface, while cultured with *E. coli* and *S. aureus* bacteria. The samples were cultured and incubated for 8 h. After incubation, lysozyme (1 mg/ml) was added and incubated further for 1 h. The solution was centrifuged for 10 min at 10000 rpm and 4 º C of temperature. The supernatant (0.5 ml) was taken in a test tube and regents such as, 0.01 M PBS (pH 7.8), 130 mM methionine, 60 μM riboflavin; 0.5 mM EDTA and 0.75 mM NBT were added. The final solution was kept in front of fluorescent light for 6 min and the absorbance was measured at 560 nm, which is directly proportional to the produced O_2^- ions [17].

Figs. 5.11 (a) and (b) represent the production of superoxides on unpolarized and polarized samples, while cultured with *E. coli* and *S. aureus* bacteria, respectively. It is observed that O_2^- production on polarized surfaces increased significantly as compared to unpolarized HA, for both, *E. coli* and *S. aureus* bacteria. The O_2^- ions, produced on the P-polarized surfaces are observed to be significantly higher than unpolarized and N-polarized surfaces of all the developed samples. It has been suggested that the O_2^- ions damage the oxidative DNA of bacterial cells by leaching of iron from proteins and enzymes, present in the media [18]. The iron oxidizes with H_2O_2 and produces the hydroxyl radicals indirectly through Fenton reaction. Those hydroxyl radicals damage the DNA of bacterial cells [19].

$$O_2^- + Fe^{3+} \rightarrow O_2 + Fe^{2+} \qquad (5.3)$$

$$H_2O_2 + Fe^{2+} \rightarrow OH^{\cdot} + OH^- + Fe^{2+} \qquad (5.4)$$

Overall, it is observed that higher amount of O_2^- ions produces on P-polarized surfaces as compared to N-polarized and unpolarized surfaces.

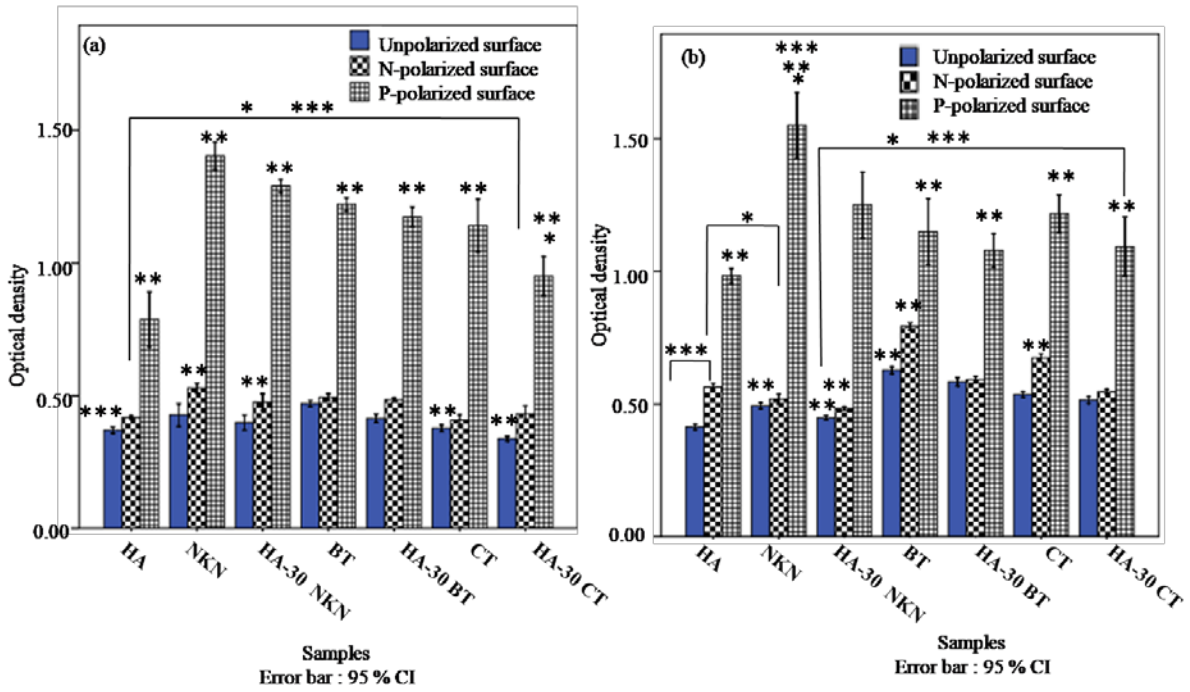

*Fig. 5.11. The super oxide production on HA, NKN, BT, CT, and HA-30 vol. % BT, HA-30 vol. % NKN, HA-30 vol. % CT composites, while cultured with (a) E. coli and (b) S. aureus bacteria. All samples show the statistically significant difference with unpolarized HA, at $p < 0.05$ (represented as *). Symbols (**) and (***) reflect the statistically significant difference among samples, while comparing with N-polarized and P-polarized HA, at $p < 0.05$, respectively.*

5.6.2. Catalase assay

The dissociation of hydrogen peroxide (H_2O_2) radicals on unpolarized and polarized sample surfaces, while cultured with *E. coli* and *S.aureus* bacteria, has been measured as catalase activity. The centrifuged culture (0.1 ml) was taken in a cuvette and 1.9 ml of phosphate buffer (pH 7.0) and 30 mM H_2O_2 were added to complete the reaction. The absorbance was taken at 240 nm. The H_2O_2, decomposed on unpolarized and polarized surfaces were calculated in terms of catalase activity/ sec [20] as,

$$\textbf{Catalase activity (K)} = \frac{\mathbf{2.3}}{\mathbf{\Delta t}} \times \mathbf{log}\frac{\mathbf{E_1}}{\mathbf{E_2}} \qquad (\mathbf{5.5})$$

Where, E_1 and E_2 are the absorbance, at t = 0 and t = 30 sec, respectively

The catalase activity for *E. coli* and *S. aureus* bacteria, while cultured on unpolarized and polarized samples are represented in Fig. 5.12. The dissociation of H_2O_2 (H_2O and O_2), protect the bacterial cells from other ROS species [21].

$$\mathbf{H_2O_2} \rightarrow \mathbf{H_2O + O_2} \qquad (\mathbf{5.6})$$

Therefore, the reduction in catalase activity increases the H_2O_2 level on surface which can damage the cell wall and DNA of bacterial cells through superoxide ions. The rate of catalase activity per sec (K) for *E. coli* and *S. aureus* bacteria, decreased significantly on polarized surfaces as compared to unpolarized surfaces for all the compositions. The maximum reduction rate in catalase activity for *E. coli* and *S. aureus* bacteria were calculated to be (78, 81, 71) % and (54, 61, 48%) on P-polarized NKN, BT and CT samples, respectively. It is observed that catalase activity/ sec (K) for both, *E. coli* and *S. aureus* bacteria are lowered on P-polarized surface which supports the MTT as well as live/ dead assay results, performed on same compositions with similar bacteria.

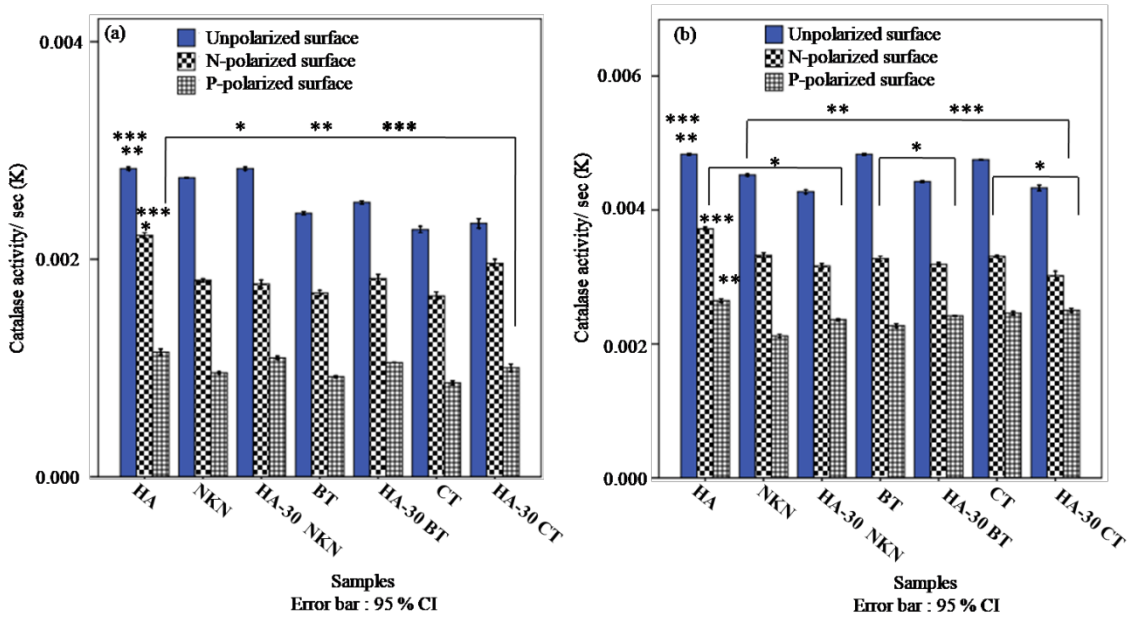

*Fig. 5.12. The catalase activity for (a) E. coli and (b) S. aureus bacteria, while cultured on HA, NKN, BT, CT, and HA-30 vol. % BT, HA-30 vol. % NKN, HA-30 vol. % CT composites. All samples show the statistically significant difference with unpolarized HA, at $p < 0.05$ (represented as *). The symbols (**) and (***) reflect the statistically significant difference among samples, while comparing with N-polarized and P-polarized HA, at $p < 0.05$, respectively.*

5.6.3 Protein estimation assay

It is used to measure the concentration of oxidized proteins in terms of protein carbonyls (n mole/mg) extracted on unpolarized and polarized sample surfaces, while cultured with *E. coli* and *S. aureus* bacteria. The concentration of protein on the cultured sample surfaces decreases with increase of the damaged bacterial cells [22]. For this assay, two reagents have been used: reagent I: (0.1 NaOH and 2 % Na_2CO_3) and reagent II: (0.5 % $CuSO_4$ and 1.35 %, potassium sodium tartrate). The reagent III was prepared using reagent I and reagent II (48 % of reagent A and 2 % of reagent B). In this assay, 20 µl of centrifuged supernatant was added in 980 µl of distilled water, which was followed by the addition of 5 ml of reagent III in the solution.

The solution was kept at room temperature for 10 min, and 500 µl of follins reagent was added for 30 min. After 30 min, the blue coloured solution was obtained. The absorbance of the solution has been measured at 750 nm [23]. The protein carbonyls for *E. coli* and *S.aureus* bacteria, cultured on unpolarized and polarized samples were calculated according to Lowery method using bovine serum albumin (BSA) as standard.

Fig.5.13 represents the protein concentration of *E. coli* and *S. aureus* bacteria, while cultured on unpolarized and polarized surfaces. The protein concentration is lowered on piezoelectric NKN, BT and CT samples than HA, which suggests that the piezoelectric NKN, BT and CT samples damage the proteins of bacterial cells. It is observed that the protein concentration significantly ($p < 0.5$) decreases with the incorporation of secondary phase in HA matrix. In addition, the protein concentration for *E. coli* and *S. aureus* bacteria was significantly ($p < 0.5$) reduced to 76, 72, 71% and 58, 64, 54 % on P-polarized NKN, BT and CT samples, respectively. The reduction in protein concentration represents the presence of free radicals that damage the cell walls as well as proteins. It is clearly observed that the protein concentration for both the bacteria reduces on P-polarized surfaces as compared to unpolarized and N-polarized surfaces which suggest the presence of higher content of free radicals on P- polarized surfaces. Overall, this assay suggests the presence of free radicals on P-polarized surfaces. In addition, this result supports the MTT as well as live/dead assays for both the bacteria.

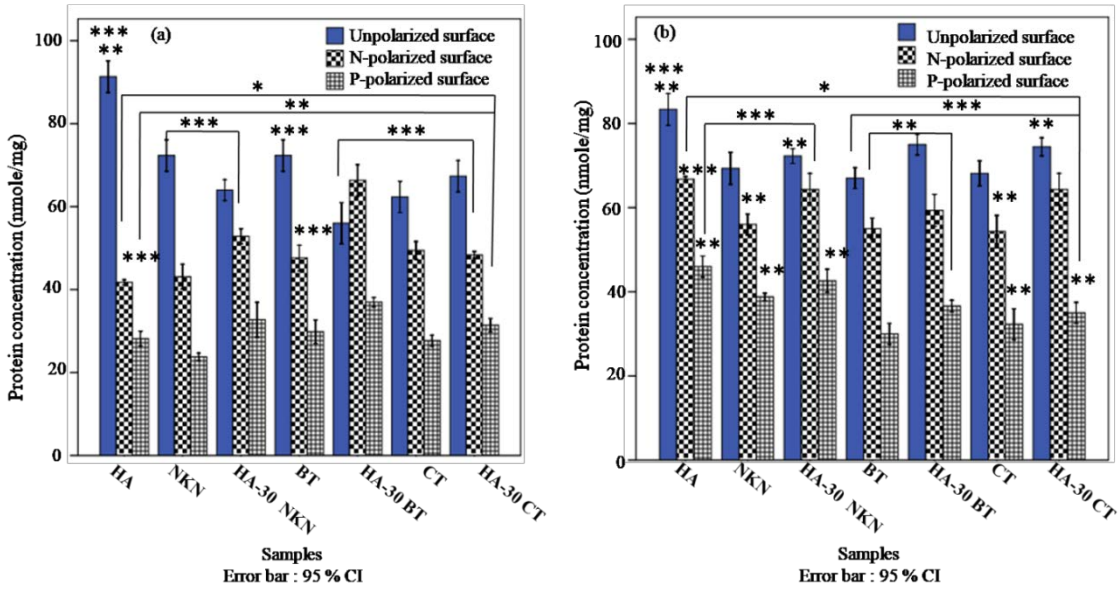

*Fig. 5.13. The concentration of protein in (a) E. coli and (b) S. aureus bacteria, while cultured on HA, NKN, BT, CT, and HA-30 vol. % BT, HA-30 vol. % NKN, HA-30 vol. % CT composites. All samples show the statistically significant difference with unpolarized HA, at $p < 0.05$ (represented as *). The symbols (**) and (***) reflect the statistically significant difference among samples, while comparing with N-polarized and P-polarized HA, at $p < 0.05$, respectively.*

5.6.4. Lipid peroxide assay (LPO assay)

LPO assay was performed to quantify the level of oxidative stress for *E. coli* and *S.aureus* bacteria, cultured on unpolarized and polarized sample surfaces. Lipoperoxidation is a chain reaction, which initiated by free radicals such as hydroxyl radicals, lipid oxyl, singlet oxygen etc. and ended up with the product of reactive aldehydes such as, malondialdehyde (MDA) and 4-hydroxynonenal (4HNE) [24]. The produced aldehydes are toxic in nature which damages the DNA and proteins in bacterial cells. In LPO assay, the supernatant (0.5 ml) was taken in test tube, containing 0.5 ml of tris HCl and incubated at 37 ºC for 2 h.

After incubation, 1 ml of trichloroacetic acid (TCA) was added. The obtained solution was centrifuged at 3500 rpm for 10 min. After centrifugation, 1.5 ml of solution was

mixed with 1.5 ml thiobarbituric acid (TBA). The final solution was boiled at 100 ºC for 10 min, which was followed by the addition of 1 ml of distilled water. The absorbance of solution has been taken at 532 nm. The LPO activity of *E. coli* and *S.aureus* bacteria was measured in terms of reactive aldehydes (end product of lipoperoxide reaction) such as, malondialdehyde, which was calculated as [25],

$$\mathbf{MDA/mg\ protein} = \frac{\mathbf{OD\ (532)\times reaction\ Volume\times 10^{9}}}{\mathbf{Sample\ volume\times 1000\times Extinsion\ coefficientof\ MDA}} \quad \textbf{(5.7)}$$

Extinsion coefficient of MDA has considered to be $1.56 \times 10^5\ \mathrm{M}^{-1}\mathrm{cm}.^{-1}$

Fig. 5.14 represents the MDA level of *E. coli* and *S. aureus* bacteria, while cultured on HA, NKN, BT, CT samples and their composite surfaces. The MDA level is directly proportional to the generation of ROS [26]. It has been observed that the MDA level for E. coli and *S. aureus* bacteria on polarized surfaces is significantly ($p < 0.5$) higher than that of unpolarized surfaces. It demonstrates that the polarized surfaces offer more ROS generation as compared to their unpolarized counterparts. The MDA level for *E. coli* and *S. aureus* bacteria significantly increased by about (63, 67, 56 %), (71, 73, 66 %) on P-polarized and (47, 55, 43 %) , (48, 49, 44 %) on N-polarized surfaces of piezoelectric NKN, BT and CT, respectively. The P-polarized surfaces demonstrate higher MDA as compared to unpolarized and N-polarized surfaces for all the compositions. In lipid peroxidation, lipids oxidize into hydroperoxides and MDA. Free radicals such as, singlet oxygen reacts with lipid hydroperoxides and breakdown into reactive lipid radicals, which can damage the cell membrane [27]. The produced MDA biologically cross-linked with DNA and proteins of bacterial cells and alter their functionality [28]. The MDA is more reactive than free radicals and react with amino acid and thiol group and consequently, damage the bacterial cells [29]. Overall, the LPO assay quantitatively supports the MTT as well as live/ dead assays for both the bacteria.

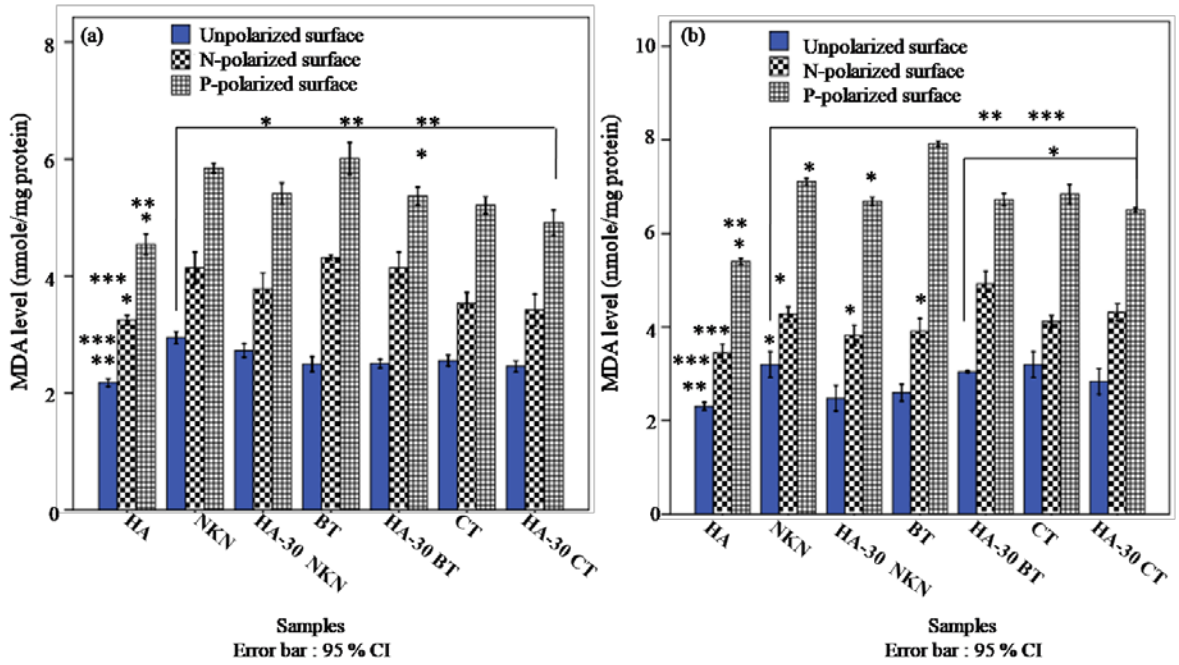

*Fig. 5.14. The produced oxidative stress in terms of MDA for (a) E. coli and (b) S. aureus bacteria, while cultured on HA, NKN, BT, CT, and HA-30 vol. % BT, HA-30 vol. % NKN, HA-30 vol. % CT composites. All the samples show the statistically significant difference with unpolarized HA at $p < 0.05$ (represented as *). The symbols (**) and (***) reflect the statistically significant difference among samples, while comparing with N-polarized and P-polarized HA at $p < 0.05$, respectively.*

5.7. Cellular response

5.7.1. MTT assay

Figs. 5.15 and 5.16 represent the MTT assay results for SaOS2 and MG-63 cells, while cultured on HA, NKN, BT, CT samples and their composite surfaces. The inclusion (30 vol. %) of NKN, BT and CT in HA enhance the total number of viable cells for both the cases. The statistical analyses reveal that all the polarized and unpolarized samples exhibit significant increase in the viability of SaOS2 and MG-63 cells in contrast to unpolarized HA, after 3, 5 and 7 days, respectively [represented as (*) in Figs. 5.15 and 5.16]. The viability of both the cells increases significantly with an increase in the duration of culture for all the developed samples (unpolarized and polarized). In relation

to polarization, both SaOS2 and MG-63 cells are more feasible on N- polarized surface as compared to unpolarized surface of the same sample [represented as (**) and (***) in Figs. 5.15 and 5.16] N-polarized HA-30 NKN demonstrates approximately 172 and 205 % increase in viability of both, SaOS2 and MG-63 cells, respectively, while cultured for 7 days. The increase in cell viability on polarized surface suggests that the ROS, produced on polarized surfaces, kills only bacterial cells and appears to promote the growth and proliferation of both, SaOS2 and MG-63 cells [30]. It has been reported that the formation of H_2O_2 produces mitogen-activated protein kinases (MAPK), Jun-N-terminal kinase (JNK) and p38 MAPK, which promote the proliferation of osteoblast-like cells [31].

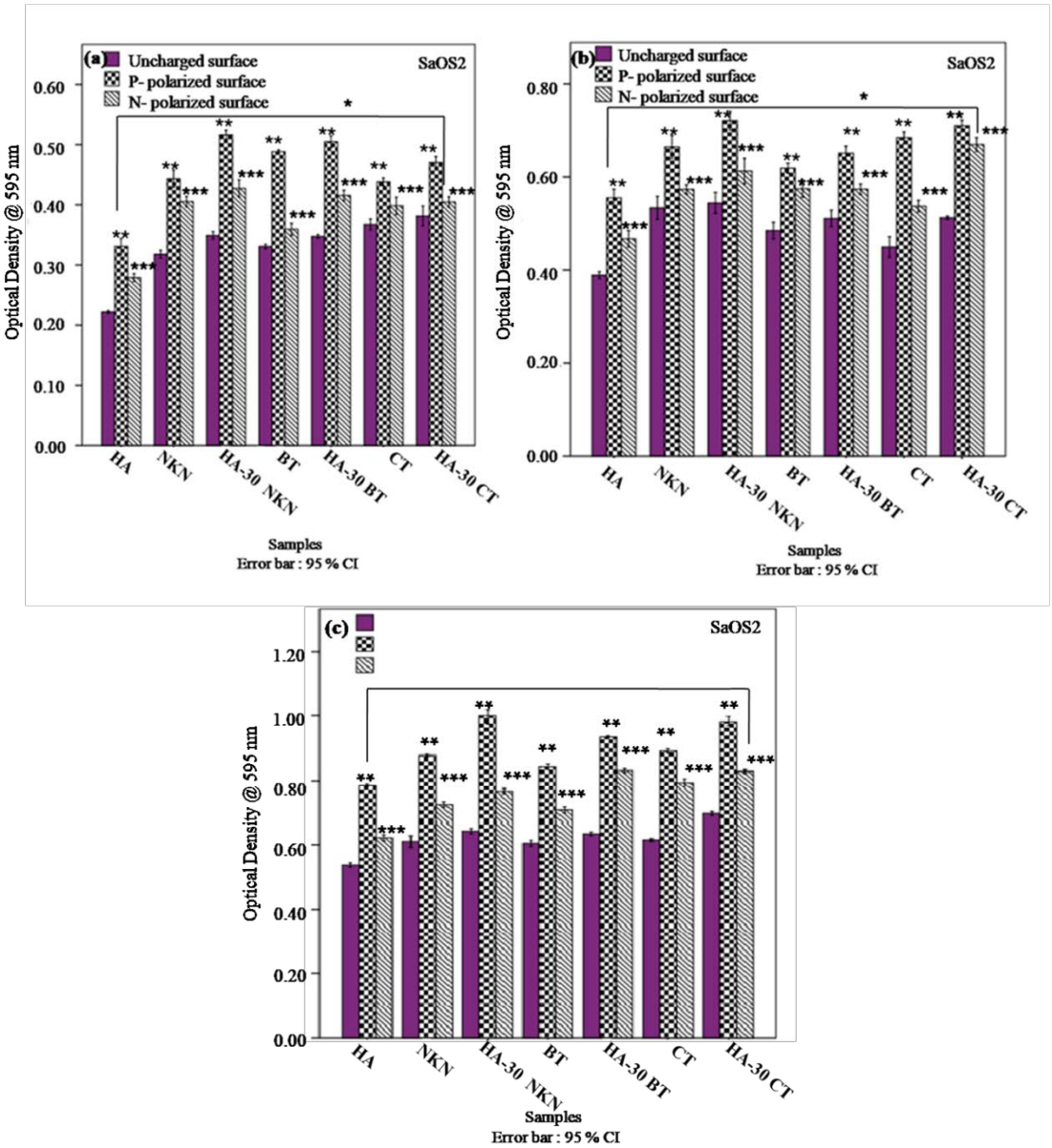

*Fig. 5.15. The Viability of SaOS2 cells, cultured on HA, NKN, BT, CT, and HA- 30 vol. % BT, HA-30 vol. % NKN, HA-30 vol. % CT composites after (a) 3, (b) 5, and (c) 7 days of incubation. All the samples show the statistically significant difference with unpolarized HA, at $p < 0.05$ (represented as *). The symbols (**) and (***) reflect the statistically significant difference among samples while comparing with N-polarized and P-polarized HA at $p < 0.05$, respectively.*

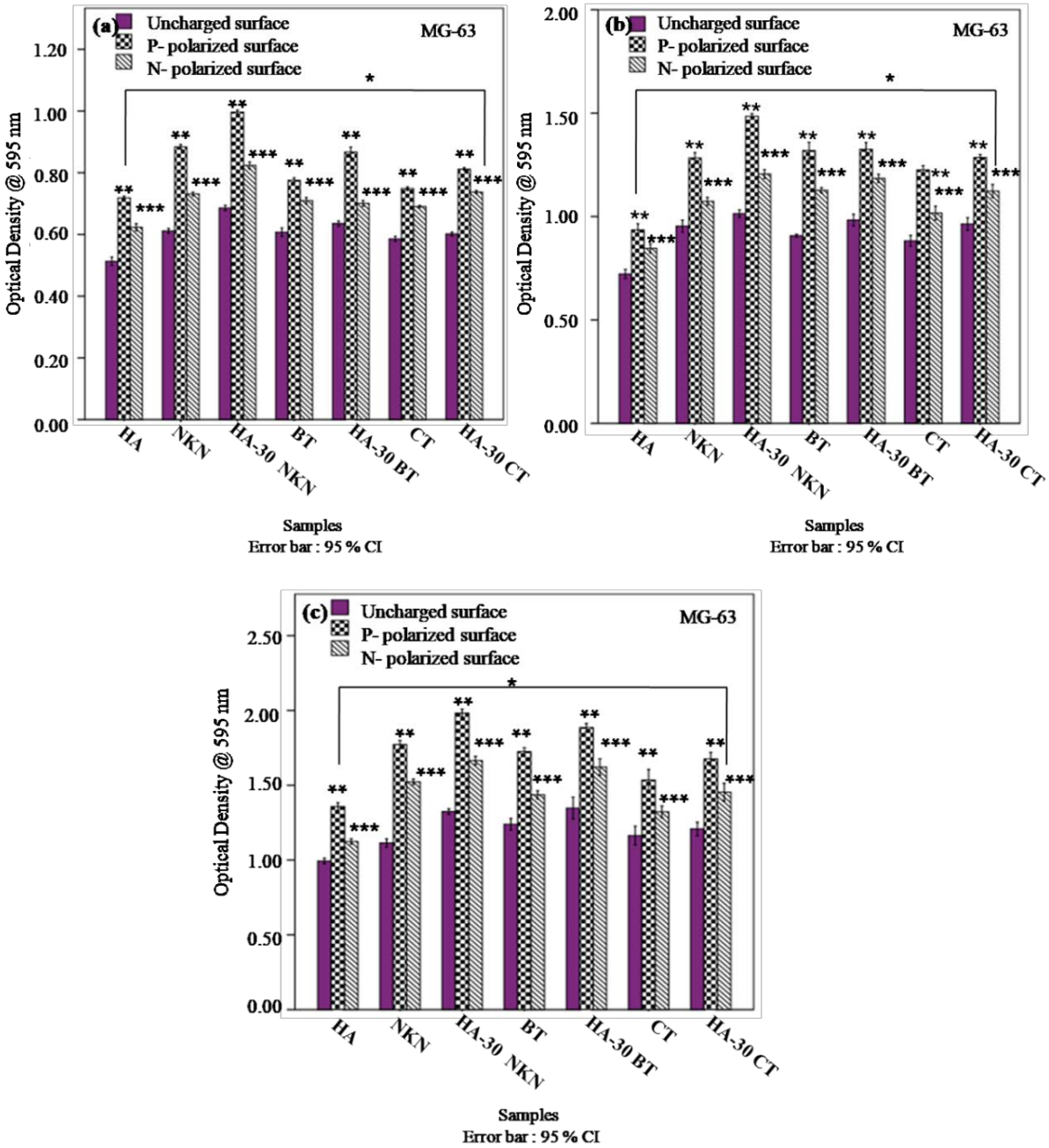

*Fig. 5.16. The Viability of MG-63 cells, cultured on HA, NKN, BT, CT, and HA-30 vol. % BT, HA-30 vol. % NKN, HA-30 vol. % CT composites after (a) 3, (b) 5, and (c) 7 days of incubation. All the samples show the statistically significant difference with unpolarized HA, at $p < 0.05$ (represented as *). The symbols (**) and (***) reflect the statistically significant difference among samples while comparing with N-polarized and P-polarized HA, at $p < 0.05$, respectively.*

5.7.2 Cell adhesion Test

Fig. 5.17 represents the morphology of MG-63 cells, while cultured on unpolarized and polarized surfaces for 3 days. It is observed that that density of MG-63 cells increases with addition of secondary phases, as compared to HA. In addition, the polarized surfaces show more cell density as compared to unpolarized surfaces of the same composition. It is observed that N-polarized surface of piezoelectric NKN, BT and their composites (HA- 30 NKN and HA-30 BT) have more adhered cells among all the samples. Overall, this result suggests that the addition of piezoelectric secondary phase as well as polarization enhances the cellular functionality.

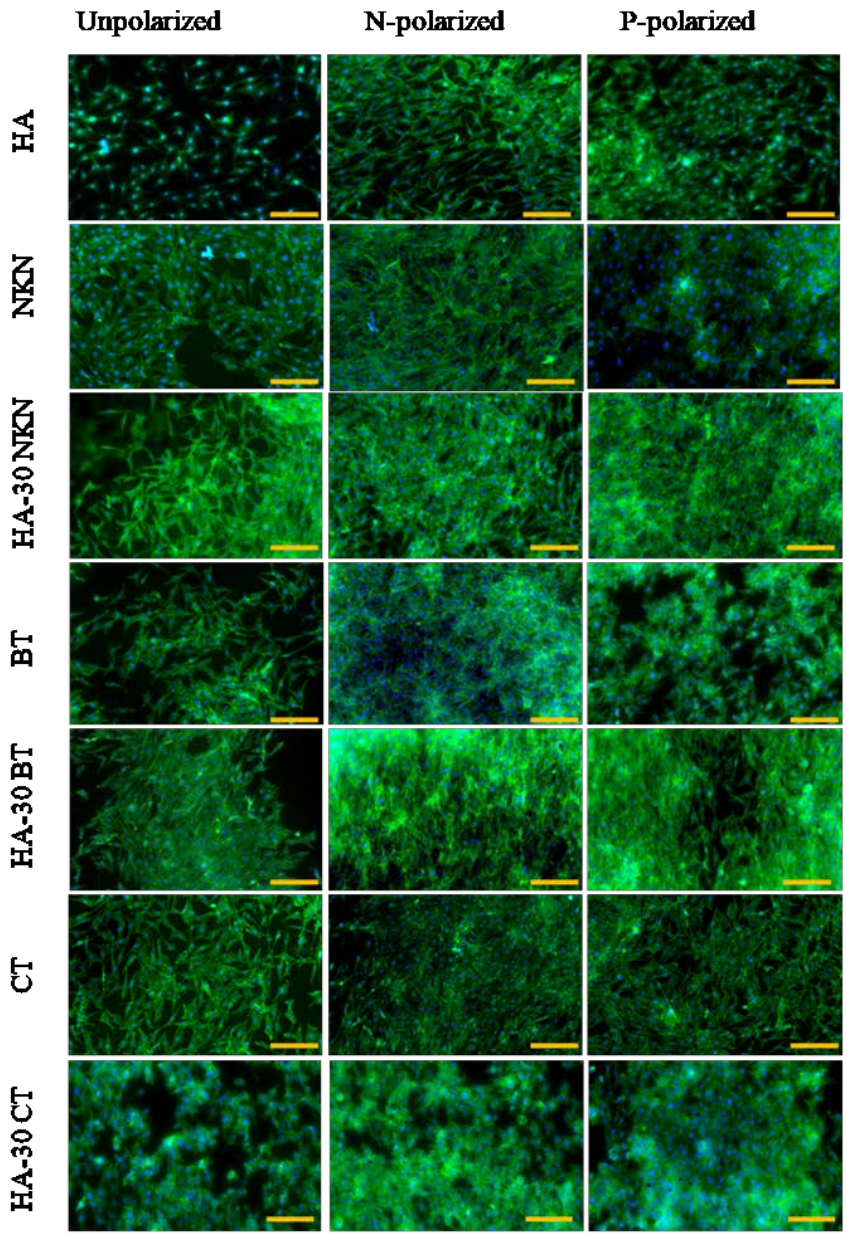

Fig. 5.17. The morphology of MG-63 cells, adhered on unpolarized and polarized HA, NKN, HA- 30 vol. % NKN, BT, HA-30 vol. % BT, CT, and HA-30 vol. % CT, after 3 days of culture (scale bar =100 µm).

It has been demonstrated that the adhesion of osteoblast-like cells on solid substrate depends on the interaction of ionic components and proteins (present in growth media) with substrate. The hydrophilicity of substrate plays an important role in initial adhesion of cells.

In addition, hydrophilic surfaces enhance the cell proliferation [32]. As discussed above, the polarization increases the hydrophilicity of both (negative and positive) surfaces. The cations such as, Ca^{+} are adsorbed of on N-polarized surfaces which interacts with the adhesion proteins and provide the favorable condition for cell growth and proliferation [33]. However, on P-polarized surfaces, anions such as HPO_4^{2-} and HCO_3^{2-} are attracted and cations get repelled, which is unfavorable for cell adhesion [34]. Fig. 5.18 illustrates the overall mechanisms, as discussed above, for antibacterial as well as cellular response on polarized surfaces.

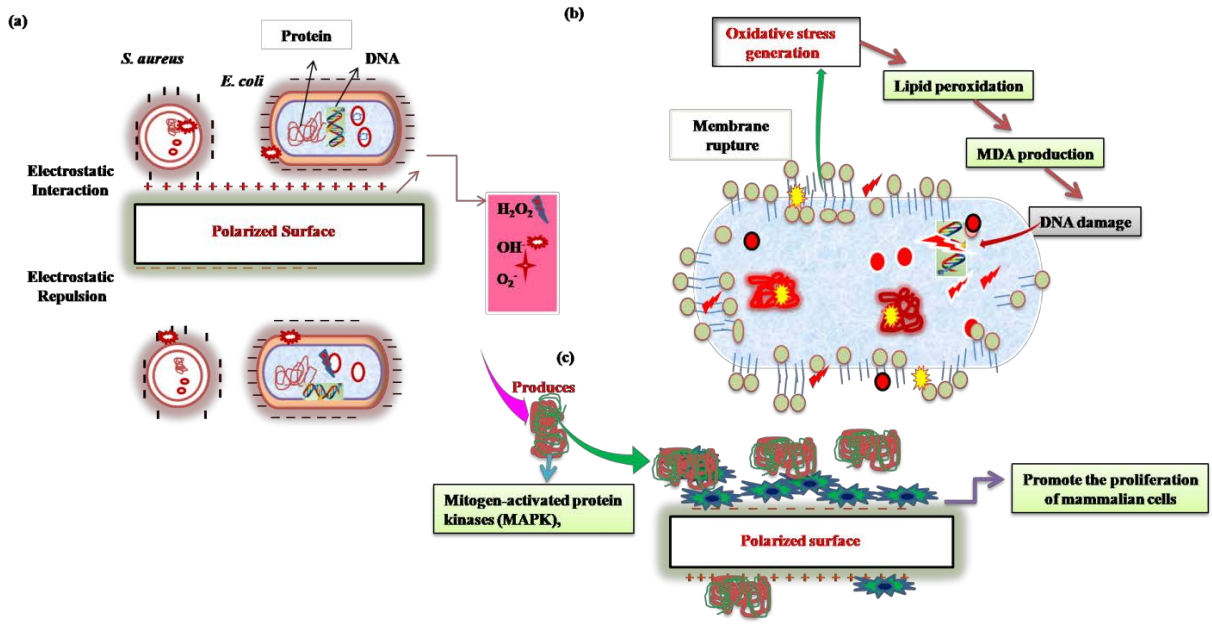

Fig. 5.18. Schematic illustrating the (a) interaction of bacteria with polarized surface, (b) mechanisms for antibacterial response of polarized surfaces, and (c) production of Mitogen-activated protein kinases (MAPK) through H_2O_2 which promote the proliferation of mammalian cells.

5.8. Closure

HA, NKN, BT, CT, HA-30 NKN, HA-30 BT and HA-30 CT composites have been successfully prepared. The XRD and FTIR reveal the formation of single-phase HA, NKN, BT, CT in their respective composites. The contact angle measurement suggests that the hydrophilicity of polarized surfaces increases as compared to that of unpolarized surfaces. The piezoelectric NKN, BT and perovskite CT exhibits antibacterial property. In addition, P-polarized NKN, BT, CT and their composites HA-30 NKN, HA-30 BT and HA-30 CT demonstrate notable reduction in viable colonies of both the bacteria in contrast to unpolarized HA. The polarized surfaces contain higher amount of ROS (superoxide's, MDA) as compared to unpolarized surfaces. Moreover, significant increase in viability of SaOS2 and MG-63 cells are observed on N-polarized surfaces of the developed composites as compared to that of HA. Overall, it has been obtained that the polarization increases the antibacterial properties of HA, NKN, BT, CT and their composites with positive impact on their cellular response.

References

1. H. Li, K.A. Khor, and P. Cheang, Effect of steam treatment during plasma spraying on the

microstructure of hydroxyapatite splats and coatings, *Journal of Thermal Spray Technology*, **15** (2006) 610-616.

2.S. Raynaud, E. Champion, D. Bernache-Assollant, P. Thomas, Calcium phosphate apatites with variable Ca/P atomic ratio I. Synthesis, characterisation and thermal stability of powders,

Biomaterials, **23** (2002) 1065–1072

3.C.L. Popa, M. Albu, C. Bartha, A. Costescu, C. Luculescu, R. Trusca, S. Antohe, Rom. Structural characterization and optical properties of hydroxyapatite/collagen matrix, *Physics Reports***, 68** (2016) 1149–1158.

4. M. D. C. B. Lopez, G. Fourlaris, B. Rand and F. L. Riley, Characterization of Barium Titanate Powders: Barium Carbonate Identification, *Journal of the American Ceramic Society*, **82** (1999) 1777–1786.

5. A. T. Chien, X. Xu, J. H. Kim, J. Sachleben, J. S. Speckand F. F. Lange, Electrical characterization of $BaTiO_3$ heteroepitaxial thin films by hydrothermal synthesis, *Journal of Materials Research and Technology*, **14** (2011) 3330–3339.

6. A. V. Polotai, A. V. Ragulya, T. V. Tomila and C. A. Randall, The XRD and IR study of the barium titanate nano-powder obtained via oxalate route, *Ferroelectrics***, 298** (2004) 243–251.

7.I. Fatimah, Y. Rahmadianti, R. A. Pudiasari, Photocatalyst of Perovskite $CaTiO_3$ Nanopowder Synthesized from CaO derived from Snail Shell in Comparison with The Use of CaO and $CaCO_3$, *Material Science and engineering*, **349** (2018) 012026.

8. ASTM International West Conshohocken, PA; Standard Test Method for Determination of Antibacterial Activity on Ceramic Surfaces *ASTM International,* (2015) doi: https://doi.org/10.1520/E3031-15.

9. L. Huang, J. Chen, X. Li, H. Liu, J. Li, T. Ren, Y. Yang, and S. Zhong, Polymethacrylic Acid Encapsulated TiO_2 Nanotubes for Sustained Drug Release And Enhanced Antibacterial Activities, *New Journal of Chemistry*, **43**, (2019); 1827-1837.

10. T. J. Beveridge, Structures of Gram-negative Cell Walls and Their Derived Membrane Vesicles, *Journal of Bacteriology*, **181** (1999) 4725–4733.

11. R. Sonohara, N. Muramatsu, H. Ohshima, T. Kondo, Difference in Surface Properties between Escherichia coli and Staphylococcus aureus as Revealed by Electrophoretic Mobility Measurements. *Biophysical chemistry,* **55** (1995) 273-7.

12. E. Kłodzińska, M. Szumski, E. Dziubakiewicz, K. Hrynkiewic, E. Skware, W. Janusz, B. Buszewsk, Effect of Zeta Potential Value on Bacterial Behavior During Electrophoretic Separation, *Electrophoresis*, **31** (2010) 1590–1596.

13. A.K. Dubey, B. Basu, Pulsed Electrical Stimulation and Surface Charge Induced Cell Growth on Multistage Spark Plasma Sintered Hydroxyapatite Barium Titanate Piezobiocomposite, *Journal of the American Ceramic Society*, **97** (2014) 481–489.

14. M.T. Ehrensberger, M.E. Tobias, S.R. Nodzo, , L.A. Hansen N.R. Luke-Marshall, L.M.; Cole, R.F. Wild, A.A. Campagnari,. Cathodic Voltage-Controlled Electrical Stimulation of Titanium Implants as Treatment for Methicillin-Resistant Staphylococcus Aureus Periprosthetic Infections, *Biomaterials*, **41** (2015) 97-105.

15. G. Tan,. S. Wang, Ye. Zhu, L. Zhou, Yu. Peng, X. Wang, He. Tianrui, C Junqi,. C. Mao, and C. Ning, Surface-Selective Preferential Production of Reactive Oxygen Species on Piezoelectric Ceramics for Bacterial Killing, *ACS Applied Materials & Interfaces*, **8** (2016) 24306–24309.

16. J. M. Slauch, How does the oxidative burst of macrophages kill bacteria Still an open question. *Molecular Microbiology,* **80(3)** (2011**)** 580–583.

17. D.Touati, M.Jacques, B.Tardat, L.Bouchard, and S. Despied, J Bacteriol.,Lethal Oxidative Damage and Mutagenesis are Generated by Iron in Delta Fur Mutants of Escherichia Coli: Protective Role of Superoxide Dismutase, *Journal of Bacteriology* **177 (9)** (1995) 2305–2314.

18. K. Keyer, Gort, A. S.; and Imlay, J. A.; Superoxide and the production of oxidative DNA damage. *Journal of Bacteriology,* **177** (1995) 6782–6790.

19. C. Beauchamp, and I. Fridovich, A Mechanism for The Production of Ethylene From Methional. The Generation of the Hydroxyl Radical By Xanthine Oxidase. *Journal of Biological Chemistry,* **245** (1970) 5214–5222.

20.H.Aebi, S.R. Wyss, B.Scherz, F. Skvaril, Eur. J. Biochem.,Heterogeneity of Erythrocyte Catalase II Isolation and Characterization of Normal and Variant Erythrocyte Catalase and Their Subunits, *European Journal of Biochemistry,* **48** (1974) 137-145.

21. R. A Greenwald, Superoxide Dismutase And Catalase as Therapeutic Agents for Human Diseases: A critical review. *Free Radical Biology and Medicine,* **8(2)** (1990), 210-219.

22.C.J. R. Thorne, Technicques in Protein and Enzyme, *Biochemistry,* (1978) 2-18

[23].O.H. Lowry, N.J. Rosebrough, A.L.Farr, and R.J.Randall, Protein Measurement with the Folin phenol reagent *Journal of Biological Chemistry*, **193** (1951) 265-275.

24. A. A.Ustinova, and V. E.Riabinin, Effect of Chronic Gamma-Irradiation on Lipid Peroxidation in CBA Mouse Blood Serum Radiat. *Radiats Biol Radioecol,* **43(4)** (2003) 459-463.

25. J.A. and S.D. Aust, Microsomal Lipid Peroxidation, *Methods in Enzymology*, **52** (1978). 302-310

26. B. Halliwell; and, M. Whiteman Measuring Reactive Species and Oxidative Damage In vivo and in Cell Culture: how should you do it and what do the results mean. *British Journal of Pharmacology, **142(*****2)*** (2004) 231-255

27. G. Sener, K. Paskaloglu, H. Toklu, C. Kapucu, A. Ayanoglu-Dulger, Kacmaz G., and A. Sakarcan, Melatonin ameliorates chronic renal failure-induced oxidative organ damage in rats. *Journal of Pineal Research*, **36(4)** (2004) 232-241.

28. A. A. Ustinova, and V. E. Riabinin, Effect of Chronic Gamma-Irradiation on Lipid Peroxidation in CBA Mouse Blood Serum. *Journal of Radiation Biology*, **43 (4)** (2003) 459-463.

29. H. A. Hassan, A. Mostafa, Lipid Peroxidation End-Products as a Key of Oxidative Stress: Effect of Antioxidant on Their Production and Transfer of Free Radicals. 2012**,** http://dx.doi.org/10.5772/45944.

30. R. Augustine, E. A. Dominic, I. Reju, B. Kaimal, N. Kalarikkal and S. Thomas. Electrospun Polycaprolactone Membranes Incorporated with ZnO Nanoparticles As Skin Substitutes With Enhanced Fibroblast Proliferation and Wound Healing, *RSC Advances*, **4** (2014) 24777.

31.Y. Zhang, L.Chen, J. Zenga, K.Zhoua, D.Zhang, Aligned Porous Barium Titanate/Hydroxyapatite Composites with High Piezoelectric Coefficients for Bone Tissue Engineering, *Materials Science and Engineering C*, **39** (2014) 143–149.

32.V. W.Wong, K. C.Rustad, J. P.Glotzbach, M.Sorkin, M.Inayathullah, M. R.Major, M. T. Longaker, J. Rajadas, G. C. Gurtner, Pullulan Hydrogels Improve Mesenchymal Stem Cell Delivery into High-Oxidative-Stress Wounds, *Macromolecular Bioscience,* **11** (2011) 1458−1466.

33. W. Chen, Y. Zunxiong, J. Pang, Y. Peng, T. Guoxin, and C. Ning, Fabrication of Biocompatible Potassium Sodium Niobate Piezoelectric Ceramic as an Electroactive Implant, *Materials (Basel)*, **10(4)** (2017) 345.

34. C. Yoshida-Noro, N. Suzuki, M.Takeichi,.Molecular Nature of The Calcium-Dependent Cell-Cell Adhesion System in Mouse Teratocarcinoma and Embryonic Cells Studied with A Monoclonal Antibody *Developmental Biology*. **101** (1984) 19–27.